AIAA JOURNAL
Vol. 45, No. 7, July 2007

Plasma Actuator Force Measurements

C. O. Porter*
U.S. Air Force Academy, USAFA, Colorado 80840
J. W. Baughn†
University of California, Davis, Davis, California 95616
and
T. E. McLaughlin,‡ C. L. Enloe,§ and G. I. Font¶
U.S. Air Force Academy, USAFA, Colorado 80840

DOI: 10.2514/1.24497

In previous work at the U.S. Air Force Academy, the phenomenology and behavior of the aerodynamic plasma actuator, a dielectric barrier discharge plasma, was investigated. To provide insight into the phenomenology associated with the transfer of momentum to air by a plasma actuator, the velocity distributions upstream and downstream of a plasma actuator with an induced boundary layer were measured using freestream velocities of approximately 4.6 and 6.8 m/s for a range of frequencies (5–20 kHz) and voltages (5–10-kV amplitude). The body forces on the air were calculated using a control volume momentum balance. In a second experiment, time-averaged results were also obtained by measuring the reaction force using a pendulum. A third experiment uses an accelerometer to gain insight into the time-dependent forces or, more specifically, the direction of the forces. The results show that the body force acts within the first 4 mm above the surface of the actuator (within the boundary layer). For a constant peak-to-peak voltage, the body force is proportional to frequency, producing a constant impulse per cycle, and the energy dissipation per cycle and efficiency are independent of frequency. The time-dependent measurements support the theory that the body force of the actuator consists of one large push followed by one small pull during each cycle.

Nomenclature

$\boldsymbol{E}$	=	electric field
e	=	electronic charge, C
F_B	=	body force
F_p	=	pressure force
F_s	=	wall shear force
f	=	frequency
N	=	ion density
P	=	pressure
q	=	dynamic pressure
$\boldsymbol{r}$	=	vector coordinates
t	=	time
u	=	velocity in the x direction
$\boldsymbol{V}$	=	velocity vector
v	=	velocity in the y direction
ρ	=	density
μ	=	viscosity

Presented at the 44th AIAA Aerospace Sciences Meeting and Exhibit, Reno, NV, 9–12 January 2006; received 7 April 2006; revision received 8 March 2007; accepted for publication 12 March 2007.

*Graduate Research Assistant, Department of Aeronautics, currently Graduate Student, University of Colorado, Colorado Springs, Department of Mechanical Engineering, Colorado Springs, CO 80933. Student Member AIAA.

†Professor, Department of Mechanical and Aeronautical Engineering, currently Distinguished Visiting Professor of Aeronautics, U.S. Air Force Academy, USAFA, CO 80840. Associate Fellow AIAA.

‡Director, Aeronautics Research Center, Faculty, Department of Aeronautics. Associate Fellow AIAA.

§Professor, Department of Physics. Senior Member AIAA.

¶Associate Professor, Department of Physics. Member AIAA.

I. Introduction

THE single-dielectric-barrier aerodynamic plasma actuator has previously been shown to transfer momentum into air, providing the potential for flow control using no moving parts. It has been extensively investigated in recent years [1–15]. The plasma actuator consists of spatially offset electrodes separated by a dielectric barrier, as shown in Fig. 1. One electrode is exposed to the air, whereas the second electrode (ground) is insulated to prevent the plasma from forming on both sides of the dielectric.

To generate the plasma, a high ac voltage (5–10-kV amplitude) is applied at a frequency ranging between 5 to 20 kHz. What forms appears to be a relatively uniform diffuse plasma discharge. However, experiments performed by Enloe et al. [16] showed that the plasma is highly structured in time and space. They also showed that for a given forcing cycle, the plasma ignites, expands, and quenches for the positive-going half of the cycle and then repeats this process for the negative-going half of the cycle. This indicates that the plasma is indeed self-limiting, in that the voltage must continually vary to sustain the plasma. Observing the temporal nature of the plasma current trace also indicates that the positive-going half of the cycle (Fig. 1b) is very irregular/patchy when compared with the negative-going half of the cycle (Fig. 1a). The difference in the two halves of the cycle suggests that there may be a difference in how they transfer momentum into the air.

The plasma actuator produces a body force on the air in the vicinity of the plasma. The body force is produced by the electric field operating on the ions of the plasma. The mean free path is extremely small (on the order of 60 nm) and the collision rate with neutral particles is extremely high (10^{10}/s). As a result, the body force essentially acts on the air as a whole, not just on the ions. Therefore, the body force is also independent of the freestream velocity, provided the flow can be assumed to be incompressible. Determining the magnitude and distribution of the body force, the effects of voltage, frequency, and induced flow velocity is important to determine the effect of the actuator on a flow.

In the presence of a flow, there is a shear force on the surface, as shown in Fig. 1. The plasma actuator body force accelerates the flow in the vicinity of the electrodes. However, the increased velocity near the surface increases the surface shear force. A reaction force exists

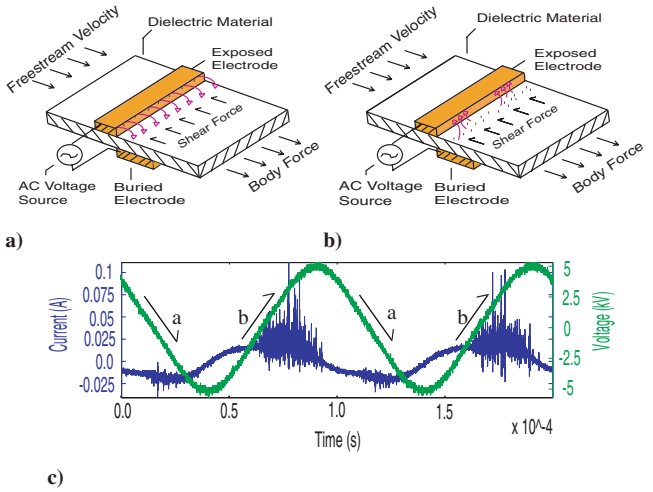

Fig. 1 Plasma actuator diagram with plasma between the offset electrodes and the differences between the discharges (Enloe et al. [16]).

on the actuator that consists of the sum of the body force and the total shear force (they act in opposite directions). In this work, measurements of this reaction force are reported in which the force is measured with a pendulum arrangement. Measurements of the body force acting on the air produced by the plasma actuator using a momentum balance on a control volume near the surface with an imposed boundary layer are also presented. The results of both of these measurements provide insight into the mechanism by which a plasma actuator transfers momentum into the air. Similarly, using the momentum balance to measure the body force allows the shear force to be quantified, which previous body-force measurements have not accounted for.

To date, two main theories exist about the temporal nature of the plasma actuator. The first theory is referred to as push–push, in which during any given cycle, the plasma actuator provides one large positive change in momentum of the air downstream of the actuator, followed by a second smaller positive increase in the momentum of the air during the opposite half of the forcing cycle. Acoustic testing previously performed by Baird et al. [17] showed two acoustic waveforms appearing per cycle, one large (probably the positive-going half of the cycle) and one small, but both apparently positive. They also observed the strong presence of a second harmonic in a power density spectral analysis. Their results supported the push–push model of the momentum transfer. Similar results were obtained from laser Doppler velocimetry (LDV) measurements by Forte et al. [18], in which a large increase in the velocity is seen, followed by possibly another increase in momentum. Finally, measurements made by Enloe et al. [13] showed that the net force obtained by using a positive and negative sawtooth waveform, which magnifies one of the discharges per cycle, was always in the same direction.

The second theory is referred to as push–pull, in which a large positive transfer of momentum into the air is seen, followed by small pull or force acting in the opposite direction of the push. Through computer simulations using particle-in-cell Monte Carlo methods, Font [19] modeled the ion-neutral interactions of the plasma over one cycle. By simulating the collisions between ions and neutrals, the average force for the positive-going half of the cycle (voltage on the exposed electrode is increasing) and the negative-going half of the cycle (voltage on the exposed electrode is decreasing) were calculated. For the negative-going half of the cycle, a negative average force was calculated, whereas the positive-going half of the cycle showed a positive force on the order of 10 times the opposite discharge. Even though the forces are in opposite directions, this still results in a net positive transfer of momentum into the air, because the average force over the entire cycle is positive (in one direction). Because an ac voltage is used, it would seem that the direction of the electric field accelerating the ions would change direction and therefore the force produced during each discharge. However, because both positive and negative ions are capable of being produced, there is a mechanism for the ions to be accelerated in the same direction, even if the electric field changes direction. However, if this is the case, this would indicate that one of the discharges is primarily producing positive ions, whereas the other discharge is producing primarily negative ions.

In an attempt to resolve the discrepancy between the measurements of Baird et al. [17] and the theoretical results of Font [19], an accelerometer was used to measure the acceleration of the actuator created in the positive-going and negative-going halves of the forcing cycle. A push–push would be indicated by two pulses per cycle (double the plasma frequency), in which the average of the pulses should average out to give the net force created by the actuator. A push–pull would be indicated by a positive acceleration for one discharge and a negative acceleration for the following discharge (identical frequency of the plasma), averaging out again to the average force created by the plasma actuator.

II. Description of the Experiments

A. Experiment 1: Body-Force Measurements Using a Momentum Balance in a Wind Tunnel

A diagram and picture of the apparatus used for this experiment are shown in Fig. 2. Electrodes were placed on opposite sides of a 3/32-in.-thick plate of glass to produce the plasma actuator. The electrodes were thin copper tape with a width of 1/4 in. for the top electrode and 1.0 in. for the bottom electrode. The bottom electrode was insulated to restrict the plasma to the top surface. The electrodes were placed so that the top electrode trailing edge was between 26 to 29 cm from the virtual start of the wind-tunnel boundary layer. The glass plate was mounted on the floor of a 12 by 12 in. test section of a wind tunnel with a freestream turbulence intensity of 1.9%. A curved fairing was added to the front of the glass plate, which extended into the inlet of the wind tunnel. A traverse device was mounted on the top

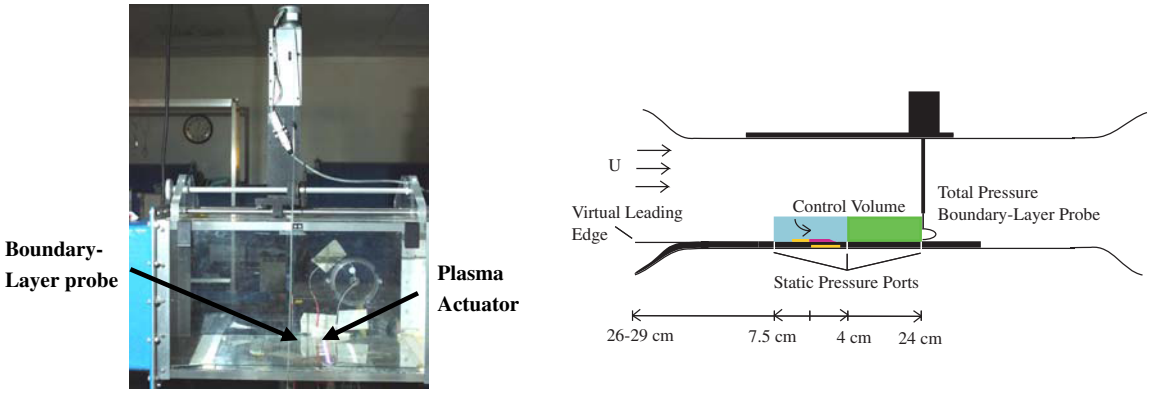

Fig. 2 Momentum balance in the wind tunnel: a) setup and b) diagram.

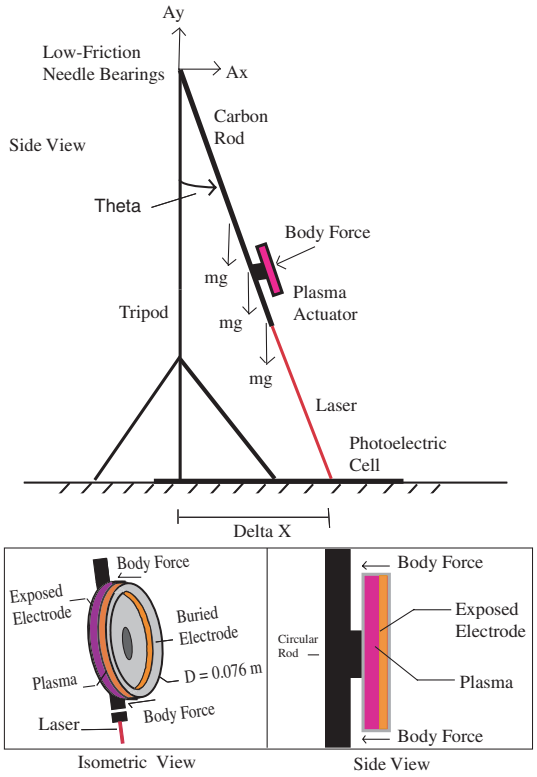

Fig. 3 Pendulum arrangement for the reaction-force measurements.

surface of the wind tunnel with a pitot boundary-layer probe. Measurements were taken at three axial locations measured from the trailing edge of the exposed electrode (−7.5, 3.5, and 7.5 cm). The measurements were made with the wind tunnel off and with two different freestream velocities (approximately 4.6 and 6.8 m/s). Four plasma-forcing frequencies were used (5, 10, 15, and 20 kHz).

A traverse device controlled with a step motor was used to position the boundary-layer pitot probe ($D = 0.625$ mm), in which one step corresponded to 0.190 mm. The difference in pressure was measured between the boundary-layer probe and a static port at each measurement location on the glass plate serving as the dielectric. The pressure was measured with a Baratron 0.2 ± 0.002 torr pressure transducer.

B. Experiment 2: Average Reaction-Force Measurements Using a Pendulum Setup

To measure the reaction force produced by the plasma actuator, a pendulum setup was used. The equations for a pendulum show that it behaves like a mass-spring-damper system, in which gravity acts as the restoring force (spring). The setup used here consisted of hanging the actuator in such a way that it acted like the bob of a pendulum.

A diagram of the pendulum setup used to measure the average force is shown in Fig. 3. Using a pendulum to measure the average body force of the plasma actuator only requires one measurement: the displacement of the pendulum. For the pendulum tests reported here, a hollow carbon rod weighing 0.938 N with a length of 1.48 m was hung from a tripod using low-friction needle bearings. A circular plasma actuator (modified petri dish with the electrodes on the outer ring of the dish) with a diameter of 0.076 m and weight of 0.304 N was placed 0.21 m from the bottom of the rod. At the end of the rod, a laser pointer weighing 0.931 N was attached such that the beam acted as an extension to the carbon rod. A photoelectric cell was placed 0.864 m below the laser pointer. As the laser pointer is displaced due to the average force of the plasma actuator, the photoelectric cell's output voltage varies due to the change in the location of the laser pointer's beam. The voltage is related to the displacement of the pendulum, and the average reaction force is determined from a moment balance for the pendulum, solving the second-order differential equation in which the damping coefficient can be found from the time-resolved displacement data.

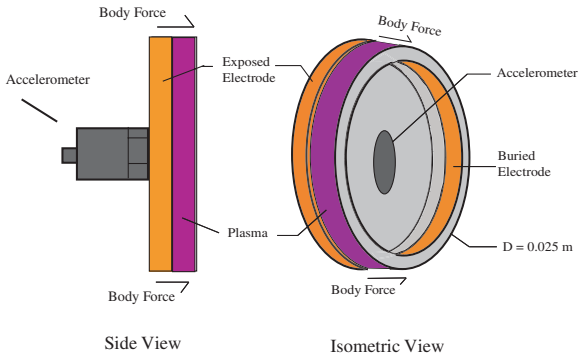

Fig. 4 Diagram of the circular actuator/accelerometer arrangement used to measure the temporal reaction force of the plasma actuator on the subcycle time scale.

C. Experiment 3: Temporal Force Measurement Using an Accelerometer Setup

To gain insight into the temporal behavior of the plasma actuator, an accelerometer was placed in the center of a different circular plasma actuator. To verify that the accelerometer was working properly, the accelerometer was mounted to a shaker (Ling Dynamic Systems Inc. V102-11710). By using a waveform generator (Agilent 33220A) hooked into an amplifier (Crown CE 1000), the signal, frequency, and amplitude input to the shaker could easily be changed. This allowed the accelerometer to be tested for sensitivity, resonant frequencies, and response time.

Figure 4 shows the diagram of the accelerometer/actuator configuration. The accelerometer was firmly mounted to a 0.0254-m-diam circular actuator (different from the circular actuator used in the pendulum arrangement). By using a circular actuator, the plasma (force) is located at a fixed radius from the accelerometer (which was mounted in the center of the actuator). This prevented any smearing of force due to the propagation speed (pressure wave traveling at the speed of sound, approximately 3000–5000 m/s in glass) when compared with the cycle time of the plasma. In other words, if the typical flat-plate plasma actuator was used, the distance between the plasma and the accelerometer would not be constant. This would result in the reaction force created during each discharge reaching the accelerometer at different times, "smearing" out the results. Using a small-diameter circular actuator also results in a resonant frequency higher than the forcing frequency of the plasma actuator. For all of the results presented here, the shell of the accelerometer was placed in a vise and the actuator was allowed to move relative to the accelerometer.

III. Results

A. Experiment 1: Momentum Balance

Measurements of the velocity profile were made on the upstream and downstream faces of the control volume, shown in Fig. 2. The area on the left is the control volume for calculations from the upstream location 7.5 cm from the trailing edge of the exposed electrode to a location 3.5 cm downstream of the trailing edge of the exposed electrode. The velocities were calculated assuming incompressible flow. It was found that the upstream velocity boundary-layer profiles were unaffected by the plasma actuator. The fact that the upstream velocity profiles do not change when the plasma is turned on means that the additional flow seen downstream (seen as the flow is accelerated near the wall surface) is sourced from the top boundary of the control volume (Fig. 2b). In essence, the actuator pulls air down from above and accelerates it downstream. This flow pattern is similar to that observed by Jacob et al. [20] using particle image velocimetry (PIV) with an imposed boundary layer. The time-averaged boundary-layer profiles for the constant power dissipated case are shown in Fig. 5. The constant power dissipated

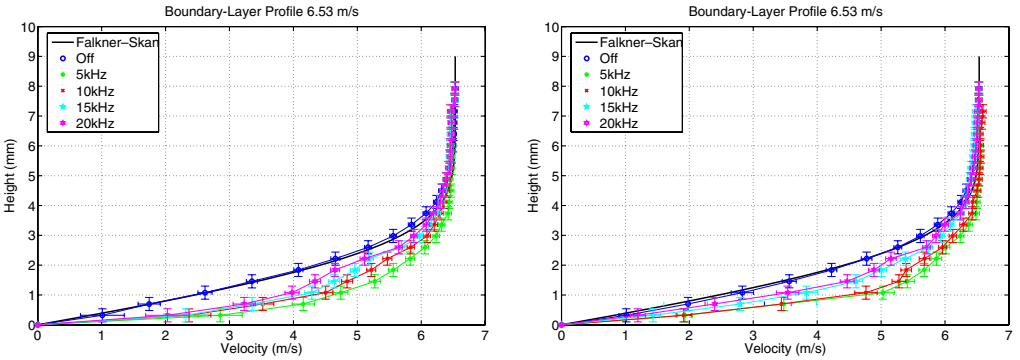

a) b)

Fig. 5 Constant power dissipated (44.0 ± 0.4 W) boundary-layer profiles: a) 3.5 cm downstream of the exposed electrode and b) 7.5 cm downstream of the exposed electrode.

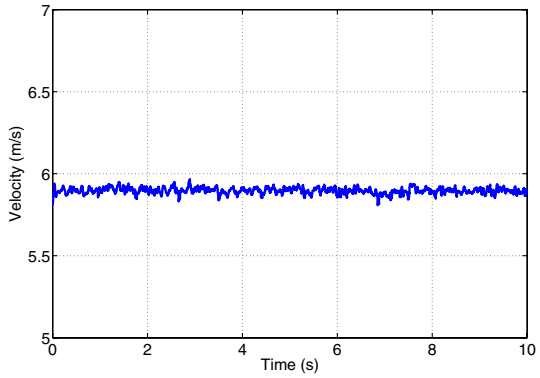

Fig. 6 Time-resolved boundary-layer measurements using a boundary-layer hot wire.

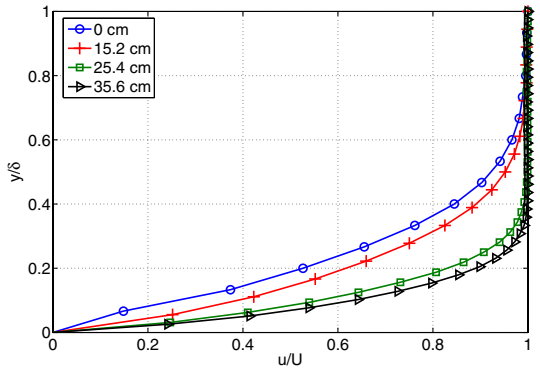

Fig. 7 Tunnel mapping showing the effects of the streamwise pressure gradient.

cases were determined by calculating the power dissipated over one complete forcing cycle, integrating the voltage and current signals. The other case in which the voltage was held constant refers to keeping the peak-to-peak voltage constant. In both cases, the ideal Falkner–Skan profile is shown for comparison to the baseline.

Time-resolved measurements of the boundary layer without the plasma, using a boundary-layer hot wire, are shown next. Figure 6 represents the velocity fluctuation inside the boundary layer at the downstream location closest to the actuator, indicating less then 2% turbulence. Furthermore, the nondimensional boundary-layer profiles throughout the test section (in the streamwise direction) are shown in Fig. 7, in which 0 cm represents the start of the test section. As shown, the wind tunnel does not provide a test section that results in self-similar boundary-layer profiles, but the shape

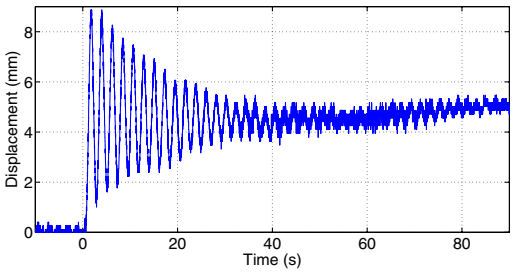

Fig. 8 Temporal nature of the plasma actuator over 90 s.

factor ($2.37 < H_{12} < 2.49$) and hot-wire measurements establish that a laminar boundary layer exists.

B. Experiment 2: Time-Averaged Reaction-Force Measurements

For each of the average body-force measurements, the plasma actuator was turned on and allowed to run for 40 s to allow the pendulum to reach a steady position. After a short time (several seconds), the displacement of the pendulum reached a steady value. It is possible to calculate the force from this displacement by noting that the sum of the moments about the pivot point of the pendulum is zero. However, due to long-term oscillations, determining the average displacement is difficult. As a result, the first two oscillations after the plasma was turned on were used to calculate the damping coefficient, and the body force could then be determined by modeling the system as a mass-spring-damper system and representing the force as a step input. The typical displacement from one of the tests is shown in Fig. 8.

During the measurements of the average force of the plasma actuator, an oscillation in the pendulum with a long period was observed. After the pendulum reached an equilibrium position and remained there for a time (about 35–40 s), the pendulum would start to oscillate in a regular fashion with a long period (100 s). Figure 8 shows the average displacement of the pendulum over a time interval of 180 s. To run the plasma actuator for such a long time interval required lowering the dissipated power to avoid breaking the glass (the dielectric) due to thermal stresses. Measurements of the plasma electrode voltage and the calculated power dissipated over this time interval were monitored and observed to be constant. Tests up to 380 s were performed, which showed this oscillation continuing at approximately 0.01 Hz. Similar tests were also performed at higher frequencies at which the oscillation was still seen, but the frequency of the oscillation slowly increased as the forcing frequency was increased from 5 to 20 kHz.

For this set of tests, the peak-to-peak voltage V_{pp} at the electrodes was held constant at 10.8 ± 0.2 kVpp, for which the uncertainty of 0.2 kV_{pp} results from the resolution of the high-voltage probe used and the A/D converter. Using this voltage, a frequency sweep was

performed using 5, 6, 7, 8.5, 10, 12, 15, and 20 kHz. To ensure that heating effects of the dielectric and the electrode did not affect the plasma, tests were performed 30 min apart to allow the actuator to cool to the ambient temperature. This also allowed the pendulum to reach its steady (equilibrium) position, such that each test was started from identical conditions. These results are discussed later, because other results are needed before interpretations can be made, and they are also compared with the momentum-balance results. Only one case is compared with the momentum-balance results, in which the peak-to-peak voltage was approximately 10 kV_{pp}. For the reaction-force measurements, the width of the buried electrode was reduced. By reducing the width of the buried electrode, the amount of surface shear stress was minimized and true body force created by the plasma actuator was obtained. To minimize the shear stress, the electrode width was selected such that the plasma extended right to the end of the buried electrode. Therefore, if the peak-to-peak voltage at the electrodes was increased, then the plasma was limited by the electrode width, reducing the volume of air that the plasma interacted with and thus reducing the body force [11].

C. Experiments 1 and 2: Body Forces

Figures 9 and 10 show the calculated body forces for the momentum-balance measurements for a constant peak-to-peak voltage and a constant power dissipated, respectively. The body force per meter of plasma was calculated as follows (using the control volume shown in Fig. 2b):

$$F_B = \Delta F_s - \int_0^{\delta} (u_{d,\text{on}} - u_{d,\text{off}})\,\mathrm{d}y + 2\int_0^{\delta} (q_{d,\text{on}} - q_{d,\text{off}})\,\mathrm{d}y \quad (1)$$

where $u_{d,\text{on/off}}$ is the velocity downstream of the actuator with the plasma on/off and $q_{d,\text{on/off}}$ is the dynamic pressure downstream of the actuator with the plasma on/off. To obtain Eq. (1), several assumption were made, starting with the integral momentum equation. The first assumption is that the flow is steady and two-dimensional. Therefore, measuring the increase in momentum at one spanwise location would give identical results if measured at a different one. The second assumption, which also allows the comparison of the momentum results to the reaction-force results, is that the extent of the plasma is a constant for a given peak-to-peak voltage, frequency, and dielectric. Finally, the body force is independent of the velocity, as discussed in the introduction. Figure 9 also contains the reaction-force measurements with the pendulum. Because the span of plasma actuator used in the pendulum setup and in the momentum-balance setup were different, the data were normalized such that the results shown represent the force produced by the plasma normalized by length. Note that there exists some region in which the body force is proportional to the frequency for all of the voltages. However, at the higher voltages and higher frequencies, the body force begins to roll off. It was noticed that at these settings, filaments began to appear in the plasma (Fig. 11).

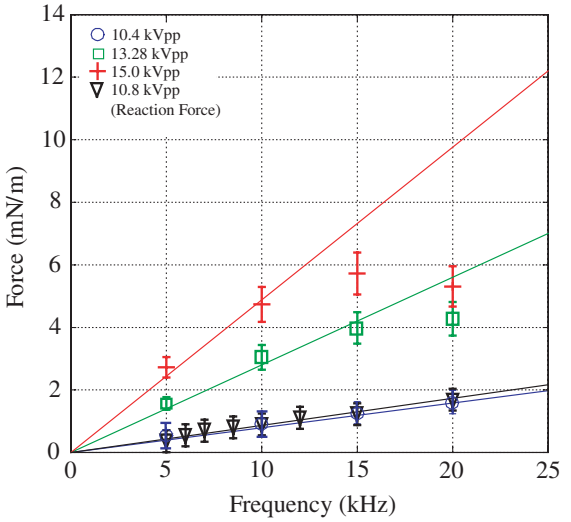

Fig. 9 Constant peak-to-peak voltage body forces.

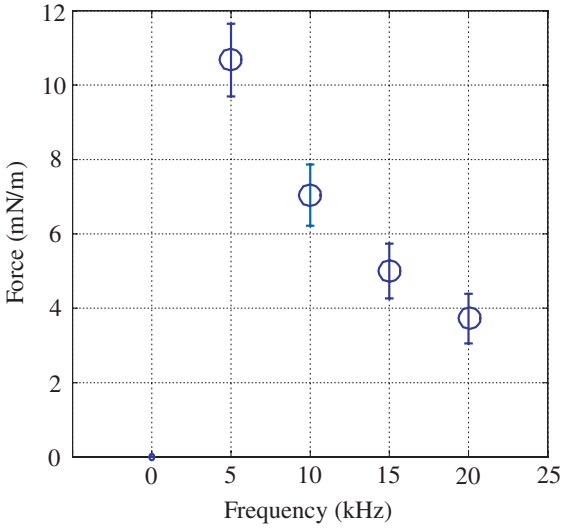

Fig. 10 Constant power dissipated (44.0 ± 0.4 W) body force.

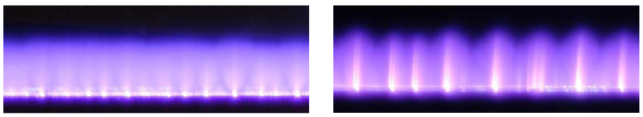

a) **b)**

Fig. 11 Plasma discharge: a) uniform and b) nonuniform with a strong presence of filaments.

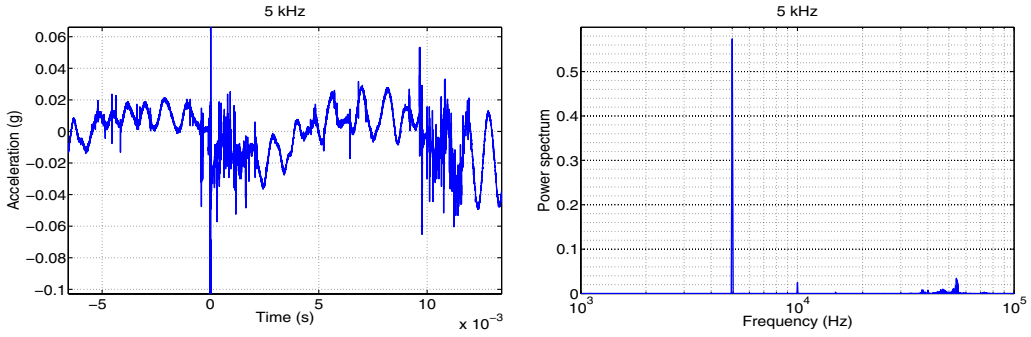

a) **b)**

Fig. 12 Accelerometer data for a plasma forcing frequency of 5 kHz: a) raw voltage signal and b) frequency spectrum.

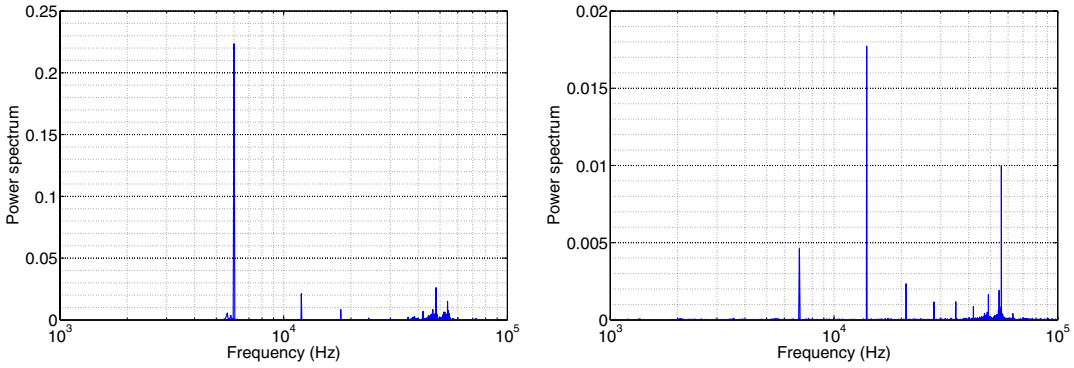

a) b)

Fig. 13 Frequency analysis of accelerometer data: a) 6 kHz and b) 7 kHz.

D. Experiment 3: Accelerometer Data

To gain insight into the direction of the force produced during each discharge of a cycle, an accelerometer was used. Because the actuator used behaves like a drum, vibrational modes are set up. To determine which part of the signal was due to vibrational modes and which part of the signal is from the force produced by the plasma actuator, the signal was decomposed into its frequency content. The goal is not to measure the amplitude of the force produced, but the direction of the force. Figure 12 shows the signal from the accelerometer for a forcing frequency of 5 kHz. The accelerometer signal was transformed into the frequency domain, as shown in Fig. 12b, which allowed us to separate any low-frequency noise, as well as the resonance of the glass, from the acceleration caused by the plasma. A primary frequency of 5 kHz is observed with a small secondary frequency of 10 kHz. Some higher resonant frequencies also appear. The frequency domains for 6- and 7-kHz forcing are shown in Fig. 13. By 7 kHz, resonant frequencies dominate the frequency spectrum, effectively corrupting the data.

IV. Discussion

A. Constant Peak-to-Peak Voltage (Experiments 1 and 2)

As shown in Fig. 9 (for constant peak-to-peak voltage), as the frequency of the plasma discharge is increased, the body force produced by the plasma also increases. In fact, the body force appears to be proportional to the frequency, at least at the lower peak-to-peak voltages and for some portion of the higher peak-to-peak voltages. These results (for the sections in which the body force varies proportionally to frequency) suggest that the body force varies linearly with frequency. At first appearance, this is somewhat surprising, because the discharge times are decreased as the frequency is increased, whereas the portion of a cycle during which a discharge occurs remains constant. The discharges can be seen in the trace of the current at the bottom of Fig. 1. Note that although the current measurements for each discharge are equal, indicating that there is an equal ionization during each discharge, photomultiplier tube (PMT) tests [16] have correlated light emissions to each of the plasma discharges, which indicates that ionization levels are not equal. This is probably due to the recombination of ions during the discharge.

If the body force is proportional to frequency (as observed, at least for some portion), then the impulse per cycle must be constant.

$$\int_0^{t\text{cycle}} F_B \mathrm{d}t = C_1 \tag{2}$$

Two explanations for a constant impulse are that either the body force must occur over only a part of the discharge, or that at higher frequencies (shorter discharge periods), the temporal body force must be higher during a discharge. It is suggested here that the second of these explanations is the more likely candidate (see Figs. 14a and 14b, in which the bottom diagrams represent a forcing frequency twice that of the forcing frequency on the top). If the power dissipated increases as the peak-to peak voltage increases, then the ion density must also increase at higher frequency, because the body force is given by

$$F_B(t) = \int_0^V N(\boldsymbol{r}, t) e \boldsymbol{E}(\boldsymbol{r}, t)\, \mathrm{d}V \tag{3}$$

where $N(\boldsymbol{r}, t)$ is the position- and time-varying ion density, and $\boldsymbol{E}$ is the position- and time-varying electric field. According to this equation, the force is proportional to the ion density and the electric field that occurs during the discharge intervals of a cycle (because

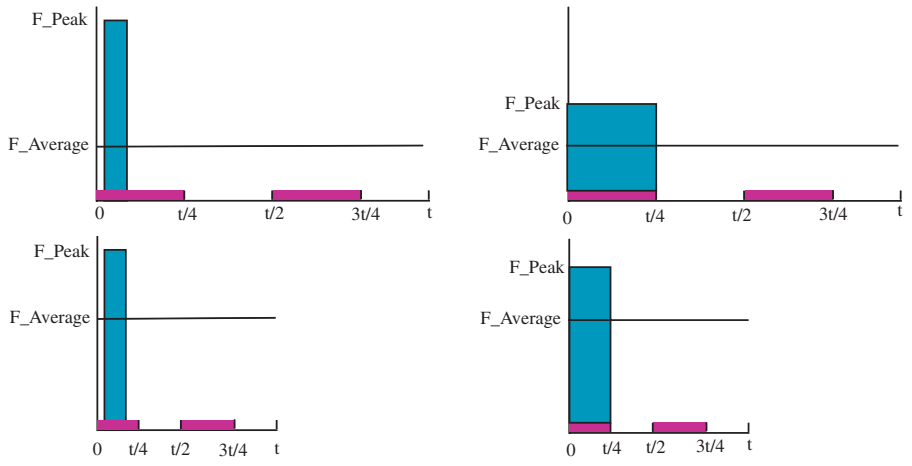

a) b)

Fig. 14 A constant impulse a) during a portion of the discharge and b) throughout the discharge.

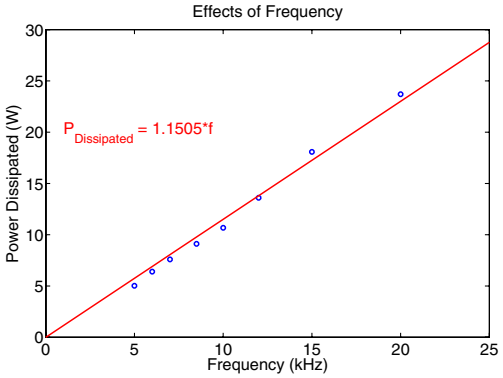

Fig. 15 Power dissipated as a function of frequency (10.8 kV_{pp}).

that is when the ions are present). If the plasma actuator works by accelerating ions, which then collide with neutrals, then as long as ions and an electric field are present, a body force must be produced. As shown by Enloe et al. [16], light emission (which is not equal for both discharges) from the plasma can be correlated to the discharges seen in the current. Therefore, it appears as if ions are present throughout the discharge, as well as an electric field, and therefore the forced produced by the plasma actuator must be continuous throughout the discharge.

If the power dissipated (at constant peak-to-peak voltage, Fig. 15) is proportional to frequency, then the efficiency is constant. The efficiency of the plasma discharge is defined by the body force divided by the power dissipated W. Because the body force appears to vary linearly with frequency and the power dissipated also appears to vary linearly (for constant peak-to-peak voltage) with frequency, then the efficiency can be found by dividing the two, which would indicate that the efficiency is constant.

This result agrees well with earlier reports (for example, Enloe et al. [21]) that suggest that the efficiency is constant at the lower forcing frequencies (up to ~12–15 kHz). Thrust measurements from Enloe et al. indicate that this appears to correspond to the region in which the body force varies linearly with frequency. However, their thrust force varies linearly with frequency, but is not proportional to the frequency, because of a slight offset (y intercept is not equal to zero). If the effects of shear force are accounted for, then the thrust would shift upward (i.e., pass through 0,0 if the shear were not reducing the net force), resulting in a proportional relationship [22]. Therefore, a linear regression can be used to determine the force ($F = C_1 \times f$) and the power dissipated ($P = C_2 \times f$). When the two are divided, the efficiency is constant (C_1/C_2). The thrust results from Enloe et al. also show that the force tends to roll off at the higher frequencies, which, as mentioned earlier, is the region in which a strong presence of filaments/streamers begin to appear. That is also the region in which the efficiency of the plasma actuator begins to decrease. This again points to the fact that obtaining a uniform filament-free discharge represents the most efficient means of the plasma actuator transferring momentum to the air, because efficiency is constant in this region.

B. Constant Power (Experiments 1 and 2)

As shown in Fig. 10, for a constant power dissipated, the body forces decrease as the frequency is increased. It is clear from Fig. 10 that if the power dissipation is held constant, the time-averaged body force will decrease substantially as the frequency is increased. This means that under these conditions, the efficiency defined as the body force divided by the power dissipation is decreasing with increasing frequency. This is a bit deceptive though, because the peak-to-peak voltage was decreased as the frequency was increased, to keep constant power. As noted earlier, if the peak-to-peak voltage is held constant, the efficiency is approximately constant.

C. Temporal Behavior (Experiment 3)

For aerodynamics applications, the time-averaged body force produced is the primary concern. This body force (discussed earlier) directly correlates to the change in momentum in the air, resulting in the potential for active flow control using a plasma actuator. However, to understand the phenomenology associated with the plasma actuator, the temporal nature of the force during a cycle is of great interest. In the following discussion, only the results for 5 and 6 kHz are used, because at higher frequencies there were resonance

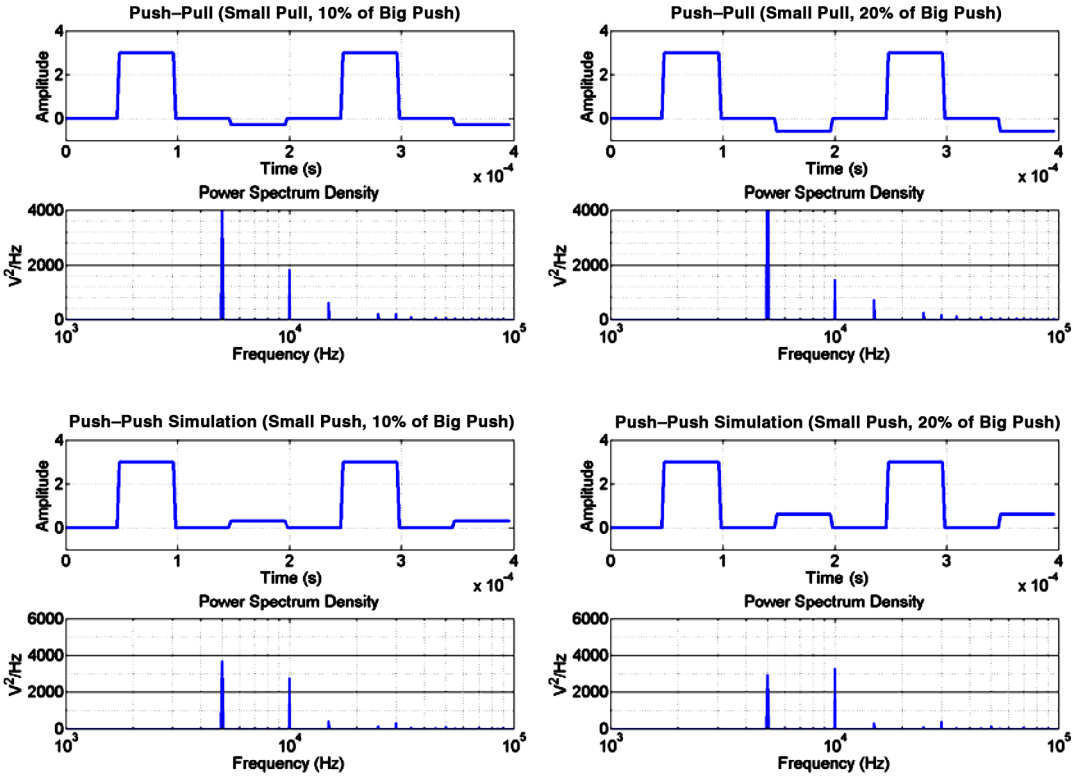

Fig. 16 Simulations of force pulses for the two different theories: push–pull and push–push and their associated frequency spectra.

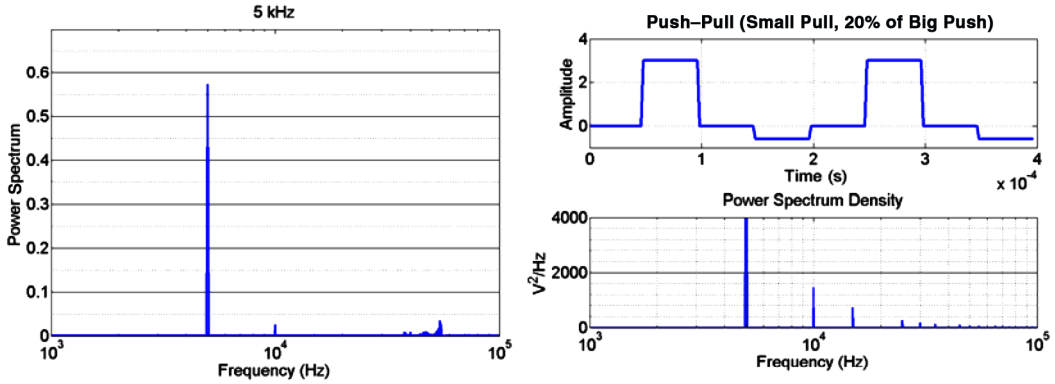

Fig. 17 Accelerometer data for 5 kHz compared with the push–pull simulation results.

issues that dominated the results (as noted in the Results section). Previous research has suggested two main theories about how the plasma actuator transfers momentum into the air. As discussed in the Introduction, one theory suggests a large push when the voltage is decreasing, followed by a small push when the voltage is increasing. The other theory suggests a push and then a pull, or body force, in the opposite direction. The accelerometer data shown in Figs. 12 and 13 can be used to support the latter theory: namely, the presence of a large push and a small pull. To illustrate this, several hypothetical force distributions (a push–push and push–pull) were assumed (from the preceding results), as shown in Fig. 16. The frequency spectra associated with each of these was calculated and are also shown in Fig. 16. The power spectrum observed in the accelerometer (a large spike at the primary frequency and small spike at twice that frequency) can only be produced if a push–pull behavior is assumed. The experimental results are compared with the hypothetical push–pull behavior in Fig. 17. This conclusion is consistent with the current theory of Font [19] that ion-neutral collisions during the secondary discharge during a cycle must produce a small push acting upstream (on the order of 10%), or what is termed a pull.

The plasma actuator is actually setting up vibrational modes in the glass plate. This is the reason that the frequency analysis is used instead of directly looking at the raw accelerometer signal or converting the signal to a force. However, this does provide a good measure of the direction of the force. If both discharges were to produce a force in the same direction, then the accelerometer would be accelerated at twice the frequency (twice per discharge), resulting in a signal in which the dominant frequency should be twice that of the actuator's forcing frequency. However, if the second discharge is in the opposite direction of the first discharge, then the dominant frequency should be identical to that of the forcing frequency, which is exactly what is seen in the signals. It should be noted that this is not conclusive, because, as shown earlier, the power spectrum at 7 kHz shows that the dominant frequency is that of 14 kHz, or twice the forcing frequency. That set of data would then suggest that both cycles were adding momentum to the flow in the same direction. However, the resonant frequency of the glass plate is between approximately 47–51 kHz. Similarly, the large spike seen at the higher frequencies occurs at 49 kHz, which would be a direct harmonic of the forcing frequency. This is evident, especially because this was not seen at the other frequencies. Unfortunately, at the higher frequencies, the forcing frequency started to approach the resonant frequencies of the accelerometer.

V. Conclusions

The body forces associated with a plasma flow actuator were investigated for a range of frequencies (from 5–20 kHz) and a range of peak-to-peak voltages (amplitude of 5–10 kV). The time-averaged body forces were measured with a pendulum arrangement and a momentum balance. The following observations were made:

1) The time-averaged body force for a constant peak-to-peak voltage is proportional to the frequency, up to a certain threshold in which a strong presence of filaments in the plasma was observed and the force began to roll off. This could suggest that obtaining the strongest plasma possible, whereas still maintaining a uniform glow discharge, represents the most efficient means of transferring momentum to the surrounding air.

2) The power dissipation for a constant peak-to-peak voltage is proportional to the frequency between 5 and 20 kHz.

3) The impulse during one cycle for a constant peak-to-peak voltage is constant (i.e., is independent of the frequency) for the range in which the force is proportional to the forcing frequency, and therefore operating the plasma at the highest frequency possible, whereas maintaining a uniform discharge for a given voltage is the most efficient means of transferring momentum.

4) The energy dissipation during one cycle for constant peak-to-peak voltage is also constant (i.e., is independent of frequency).

5) The efficiency of the plasma actuator (force/power) for constant peak-to-peak voltage is therefore constant (i.e., independent of frequency when the force is proportional to the forcing frequency).

6) Accelerometer data (which can be interpreted as the temporal force) support the theory of Font [19] that the plasma actuator produces one large push and one small pull (force in the opposite direction) during a cycle.

7) The time interval for the discharges decreases as the frequency is increased, but remains a constant fraction of the total cycle time.

8) With an imposed boundary layer (wind tunnel on-flow on a flat plate) the air near the surface (within 4 mm) is accelerated. From momentum conservation, it was found that most of the air accelerated comes from above the actuator, consistent with both PIV measurements [20] and LDV measurements [18].

9) The accelerated air near the surface increases the velocity gradient and surface shear stress. Therefore, any measurements of the body force produced must account for this added shear force.

10) With an imposed boundary layer, the boundary-layer velocity distribution a short distance (7.5 cm) upstream of the plasma is unaffected by the plasma.

11) As flow continues downstream from the actuator, the momentum increase provided by the plasma actuator diffuses and is decreased by surface shear.

12) For a constant power, the body force and efficiency decrease as the frequency is increased from 5 to 20 kHz.

Acknowledgments

The authors gratefully acknowledge the support of the U.S. Air Force Office of Scientific Research and John Schmisseur, program manager, for the work presented here. The authors also appreciate early attempts by Corrie Baird to set up a pendulum arrangement for the measurement of the plasma actuator force. Author C. O. Porter appreciates the academic guidance of Jason Roney at the University of Colorado, where he is pursuing his Master's degree. Author J. W. Baughn appreciates the support of the Distinguished Visiting Professor program at the U.S. Air Force Academy and the help of John Sherfesee, director of this program.

References

[1] List, J., Byerley, A. R., McLaughlin, T. E., and Van Dyken, R., "Using Plasma Actuators Flaps to Control Laminar Separation on Turbine Blades in a Linear Cascade," 41st Aerospace Sciences Meeting and Exhibit, Reno, NV, AIAA Paper 2003-1026, 2003.

[2] Huang, J., Corke, T., and Thomas, F., "Plasma Actuators for Separation Control of Low Pressure Turbine Blades," 41st Aerospace Sciences Meeting and Exhibit, Reno, NV, AIAA Paper 2003-1027, 2003.

[3] Corke, T. C., and Matlis, E., "Phased Plasma Arrays for Unsteady Flow Control," Fluids 2000 Conference, Denver CO, AIAA Paper 2000-2323, 2000.

[4] Post, M. L., and Corke, T. C., "Separation Control of High Angle of Attack Airfoil Using Plasma Actuators," 41st Aerospace Sciences Meeting and Exhibit, Reno, NV, AIAA Paper 2003-1024, 2003.

[5] Corke, T. C., Jumper, E. J., Post, M. L., Orlov, D., and McLaughlin, T. E., "Application of Weakly-Ionized Plasmas as Wing Flow Control Devices," 40th Aerospace Sciences Meeting and Exhibit, AIAA Paper 2002-0350, 2002.

[6] Roth, J. R., Sherman, D. M., and Wilkinson, S. P., "Boundary Layer Flow Control with a One Atmosphere Uniform Glow Discharge Surface Plasma," 36th Aerospace Sciences and Exhibit, Reno, NV, AIAA Paper 98-0328, 1998.

[7] Roth, J. R., Sherman, D. M., and Wilkinson, S. P., "Electrohydrodynamic Flow Control with a Glow-Discharge Surface Plasma," *AIAA Journal*, Vol 38, No. 7, July 2000, pp. 1166–1172.

[8] Roth, J. R., Sin, H., Chandra, R., and Madhan, M., "Flow Reattachment and Acceleration by Paraelectric and Peristaltic Electrohydrodynamic (EHD) Effects," 41st Aerospace Sciences Meeting and Exhibit, Reno, NV, AIAA 2003-0531, 2003.

[9] Wilkinson, S., "Investigation of an Oscillating Surface Plasma for Turbulent Drag Reduction," 41st Aerospace Sciences Meeting and Exhibit, Reno, NV, AIAA Paper 2003-1023, 2003.

[10] Ashpis, D., and Hultgren, L., "Demonstration of Separation Delay with Glow Discharge Plasma Actuators," 41st Aerospace Sciences Meeting and Exhibit, Reno, NV, AIAA Paper 2003-1025, 2003.

[11] VanDyken, R., McLaughlin, T. E., and Enloe, C. L., "Parametric Investigation of a Single Dielectric Barrier Plasma Actuator," 42nd Aerospace Sciences Meeting and Exhibit, Reno, NV, AIAA Paper 2004-0846, 2004.

[12] Asghar, A., and Jumper, E. J., "Phased Synchronization of Vortex Shedding from Multiple cylinders Using Plasma Actuators," 41st Aerospace Sciences Meeting and Exhibit, Reno, NV, AIAA Paper 2003-1028, 2003.

[13] Enloe, C. L., McLaughlin, T. E., Van Dyken, R. D., Kachner, K. D., Jumper, E. J., Corke, T. C., Post, M. L., and Haddad, O., "Mechanisms and Responses of a Single Dielectric Barrier Discharge Plasma Actuator: Geometric Effects," *AIAA Journal*, Vol. 42, No. 3, Mar. 2004, pp. 595–604.

[14] Enloe, C. L., McLaughlin, T. E., Van Dyken, R. D., Kachner, K. D., Jumper, E. J., and Corke, T. C., "Mechanisms and Responses of a Single Dielectric Barrier Discharge Plasma Actuator: Plasma Morphology," *AIAA Journal*, Vol 42, No. 3, Mar. 2004, pp. 589–594.

[15] Enloe, C. L., McLaughlin, T. E., Van Dyken, R. D., Kachner, K. D., Jumper, E. J., and Corke, T. C., "Mechanisms and Responses of a Single Dielectric Barrier Plasma," 41st Aerospace Sciences Meeting and Exhibit, Reno, NV, AIAA Paper 2003-1021, 2003.

[16] Enloe, C. L., McLaughlin, T. E., Font, G. I., and Baughn, J. W., "Parameterization of Temporal Structure in the Single Dielectric Barrier Aerodynamic Plasma Actuator," 43rd Aerospace Sciences Meeting and Exhibit, Reno, NV, AIAA Paper 2005-0564, 2005.

[17] Baird, C., Enloe, C. L., McLaughlin, T. E., and Baughn, J. W., "Acoustic Testing of the Dielectric Barrier Discharge (DBD) Plasma Actuator," 43rd Aerospace Sciences Meeting and Exhibit, Reno, NV, AIAA Paper 2005-0565, 2005.

[18] Forte, M., Jolibois, J., Moreau, E., and Touchard, G., "Optimization of a Dielectric Barrier Discharge Actuator by Stationary and Non-Stationary Measurements of the Induced Flow Velocity—Application to Airflow Control," 3rd AIAA Flow Control Conference, San Francisco CA, AIAA Paper 2006-2863, 2006.

[19] Font, G. I., "Boundary Layer Control with Atmospheric Plasma Discharges," 40th AIAA/ASMA/SAE/ASEE Joint Propulsion Conference and Exhibit, Fort Lauderdale, FL, AIAA Paper 2004-3574, 2004.

[20] Jacob, J., Rivir, R., and Carter, C., "Boundary Layer Flow Control Using ac Discharge Plasma Actuators," 2nd AIAA Flow Control Conference, Portland, OR, AIAA Paper 2004-2128, 2004.

[21] Enloe, C. L., McLaughlin, T. E., Font, G. I., and Baughn, J. W., "Parameterization of Temporal Structure in the Single Dielectric Barrier Aerodynamic Plasma Actuator," *AIAA Journal*, Vol. 44, No. 6, June 2006, pp. 1127–1136.

[22] Enloe, C. L., McLaughlin, T. E., Font, G. I., and Baughn, J. W., "Frequency Effects on the Efficiency of the Aerodynamic Plasma Actuator," 44th AIAA Aerospace Sciences Meeting and Exhibit, Reno, NV, AIAA Paper 2006-166, 2006.

M. Auweter-Kurtz
Associate Editor